Measuring KS0K± interactions using pp collisions at s=7 TeV

EUROPEAN ORGANIZATION FOR NUCLEAR RESEARCH

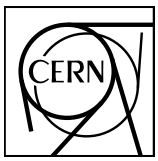

CERN-EP-2018-234
29 August 2018

Measuring $K^0_S K^\pm$ interactions using pp collisions at $\sqrt{s} = 7$ TeV

ALICE Collaboration*

Abstract

We present the first measurements of femtoscopic correlations between the K^0_S and $K^\pm$ particles in pp collisions at $\sqrt{s} = 7$ TeV measured by the ALICE experiment. The observed femtoscopic correlations are consistent with final-state interactions proceeding solely via the $a_0(980)$ resonance. The extracted kaon source radius and correlation strength parameters for $K^0_S K^-$ are found to be equal within the experimental uncertainties to those for $K^0_S K^+$. Results of the present study are compared with those from identical-kaon femtoscopic studies also performed with pp collisions at $\sqrt{s} = 7$ TeV by ALICE and with a $K^0_S K^\pm$ measurement in Pb-Pb collisions at $\sqrt{s_{\rm NN}} = 2.76$ TeV. Combined with the Pb-Pb results, our pp analysis is found to be compatible with the interpretation of the $a_0(980)$ having a tetraquark structure instead of that of a diquark.

*See Appendix A for the list of collaboration members

1 Introduction

Recently, by using Pb-Pb collisions at $\sqrt{s_{\rm NN}} = 2.76$ TeV, the ALICE experiment [1] has published the first-ever study of $K^0_S K^\pm$ femtoscopy [2]. $K^0_S K^\pm$ femtoscopy differs from identical-kaon femtoscopy, for which a number of studies exist in the literature [3–6], in that the only pair interaction expected is a final-state interaction (FSI) through the $a_0(980)$ resonance. It was found in that Pb-Pb study that the FSI in $K^0_S K^\pm$ proceeds solely through the $a_0(980)$ resonance, i.e. with no competing non-resonant channels, and the extracted kaon source parameters agree with published results from identical-kaon studies in Pb-Pb collisions. These results were found to be compatible with the interpretation of the a_0 resonance as a tetraquark state rather than a diquark[1] state [2, 7–9]. A recent theoretical calculation has shown that the ALICE Pb-Pb results can indeed be described by a model based on the four-quark model [10].

The argument given in Ref.[2] for a tetraquark a_0 being compatible with the Pb-Pb $K^0_S K^\pm$ result stated above is based on two factors: 1) the kaon source geometry, and 2) an empirical selection rule (For the sake of simplicity of notation, "a_0" will be used for the remainder of this paper to represent "$a_0(980)$."). For factor 1), the production cross section of the a_0 resonance in a reaction channel such as $K^0 K^- \to a_0^-$ should depend on whether the a_0^- is composed of $d\overline{u}$ or $d\overline{s}s\overline{u}$ quarks, the former requiring the annihilation of the $\overline{s}s$ pair and the latter being a direct transfer of the valence quarks from the kaons to the a_0^-. Since the femtoscopic size of the 0-10% most central Pb-Pb collision is measured to be 5–6 fm, the large geometry in these collisions is favorable for the direct transfer of quarks to the a_0, whereas not favorable for the annihilation of the strange quarks due to the short-ranged nature of the strong interaction. For factor 2), the direct transfer of the valence quarks from the kaons to the a_0^- is favored since this is an "OZI superallowed" reaction [9]. The OZI rule can be stated as "an inhibition associated with the creation or annihilation of quark lines" [9]. Thus, the annihilation of the strange quarks is suppressed by the OZI rule. Both of these factors favor the formation of a tetraquark a_0 and suppress the formation of a diquark a_0. As a result of this, if the a_0 were a diquark, one would expect competing non-resonant channels present and/or no FSI at all, i.e. free-streaming, of the kaon pair thus diluting the strength of the a_0 resonant FSI. The fact that this is not seen to be the case in Pb-Pb collisions favors the tetraquark a_0 interpretation.

The geometry of the kaon source is seen to be an important factor in the argument given above, i.e. the large kaon source seen in Pb-Pb collisions suppresses the annihilation of the strange quarks in the kaon pair and enhances the direct transfer of quarks to the a_0. It is interesting to speculate on the dependence of the strength of the a_0 resonant FSI on the size of the kaon source, particularly for a very small source of size ~ 1 fm that would be obtained in pp collisions [4, 5]. For a kaon source of size ~ 1 fm, the kaons in a produced kaon pair would be overlapping with each other at the source, thus giving a geometric enhancement of the strange-quark annihilation channel that could compete with, or even dominate over, the OZI rule suppression of quark annihilation. Thus we might expect that the tetraquark a_0 resonant FSI could be diluted or completely suppressed by competing non-resonant annihilation channels that could open up, whereas a diquark a_0 resonant FSI, which was not seen to be suppressed by either geometry or the OZI rule in Pb-Pb, would not be diluted. A femtoscopic measurement of $K^0_S K^\pm$ correlations in pp collisions should be able to test this by determining the strength of the a_0 FSI by measuring the femtoscopic λ parameter. In more concrete terms, if we were to compare the λ parameters extracted in $K^0_S K^\pm$ femtoscopic measurements in pp collisions and Pb-Pb collisions, for a tetraquark a_0 we would expect $\lambda_{K^0_S K^\pm(\rm PbPb)} > \lambda_{K^0_S K^\pm(\rm pp)}$ whereas for a diquark a_0 we would expect $\lambda_{K^0_S K^\pm(\rm PbPb)} \sim \lambda_{K^0_S K^\pm(\rm pp)}$. An independent check could also be made by comparing λ from $K^0_S K^\pm$ femtoscopy in pp collisions with λ from identical-kaon femtoscopy in pp collisions in a similar way as was done for Pb-Pb collisions [2]. Since we expect identical-kaon correlations to go solely through quantum statistics (and FSI for neutral kaons), our expectation for a tetraquark a_0 would be $\lambda_{KK(\rm pp)} > \lambda_{K^0_S K^\pm(\rm pp)}$ whereas for a diquark a_0 we would expect $\lambda_{KK(\rm pp)} \sim \lambda_{K^0_S K^\pm(\rm pp)}$.

[1] Note that the term "diquark" will be used in this paper to indicate a $q_i\overline{q}_j$ quark pair.

In this Letter, femtoscopic correlations with the particle pair combinations $K^0_S K^\pm$ are studied for the first time in pp collisions at $\sqrt{s} = 7$ TeV by the ALICE experiment. The physics goals of the present $K^0_S K^\pm$ femtoscopy study are the following: 1) show to what extent the FSI through the a_0 resonance describes the correlation functions, 2) study the K^0 and $\overline{K}^0$ sources to see if there are differences in the source parameters, 3) compare the results of the extracted kaon source parameters from the present study with the published results from Pb-Pb collisions and identical kaon results from pp collisions, and 4) see if the results from this pp study are compatible with a tetraquark a_0 as suggested from the Pb-Pb study.

2 Description of experiment and data selection

The ALICE experiment and its performance in the LHC Run 1 $(2009-2013)$ are described in Ref. [1] and Ref. [11, 12], respectively. About 370×10^6 minimum-bias 7 TeV pp collision events taken in 2010 were used in this analysis. Events were classified using the measured amplitudes in the V0 detectors, which consist of two arrays of scintillators located along the beamline and covering the full azimuth [13, 14]. Charged particles were reconstructed and identified with the central barrel detectors located within a solenoid magnet with a field strength of $B = \pm 0.5$ T. Charged particle tracking was performed using the Time Projection Chamber (TPC) [15] and the Inner Tracking System (ITS) [1]. The ITS allowed for high spatial resolution in determining the primary (collision) vertex. A momentum resolution of less than 10 MeV/c was typically obtained for the charged tracks of interest in this analysis [16]. The primary vertex was obtained from the ITS, the position of the primary vertex being constrained along the beam direction (the "z-position") to be within ± 10 cm of the center of the ALICE detector. In addition to the standard track quality selections [16], the selections based on the quality of track fitting and the number of detected tracking points in the TPC were used to ensure that only well-reconstructed tracks were taken in the analysis [11, 15, 16].

Particle identification (PID) for reconstructed tracks was carried out using both the TPC and the Time-of-Flight (TOF) detectors in the pseudorapidity range $|\eta| < 0.8$ [11, 12]. For the PID signal from both detectors, a value was assigned to each track denoting the number of standard deviations between the measured track information and calculated values (N_σ) [6, 11, 12, 16]. For TPC PID, a parametrized Bethe-Bloch formula was used to calculate the specific energy loss $\langle \mathrm{d}E/\mathrm{d}x \rangle$ in the detector expected for a particle with a given mass and momentum. For PID with TOF, the particle mass was used to calculate the expected time-of-flight as a function of track length and momentum. This procedure was repeated for four "particle species hypotheses", i.e. electron, pion, kaon and proton, and, for each hypothesis, a different N_σ value was obtained per detector.

2.1 Kaon selection

The methods used to select and identify individual K^0_S and $K^\pm$ particles are the same as those used for the ALICE $K^0_S K^0_S$ [4] and $K^\pm K^\pm$ [5] analyses from $\sqrt{s} = 7$ TeV pp collisions. These are now described below.

2.1.1 K^0_S selection

The K^0_S particles were reconstructed from the decay $K^0_S \to \pi^+\pi^-$, with the daughter π^+ and π^- tracks detected in the TPC, ITS and TOF detectors. The secondary vertex finder used to locate the neutral kaon decays employed the "on-the-fly" reconstruction method [16], which recalculates the daughter track momenta during the original tracking process under the assumption that the tracks came from a decay vertex instead of the primary vertex. Pions with $p_\mathrm{T} > 0.15$ GeV/c were accepted (since for lower p_T track finding efficiency drops rapidly) and the distance of closest approach to the primary vertex (DCA) of the reconstructed K^0_S was required to be less than 0.3 cm in all directions. The required N_σ values for the pions were $N_\sigma^\mathrm{TPC} < 3$ (for all momenta) and $N_\sigma^\mathrm{TOF} < 3$ for $p > 0.8$ GeV/c. An invariant mass distribution for the $\pi^+\pi^-$ pairs was produced and the K^0_S was defined to be resulting from a pair that fell

into the invariant mass range $0.480 < m_{\pi^+\pi^-} < 0.515$ GeV/c^2, corresponding to $\pm 4.7\sigma$, where $\sigma = 3.7$ MeV/c^2 is the width of a Gaussian fit to the invariant mass distribution.

2.1.2 $K^\pm$ selection

Charged kaon tracks were detected using the TPC and TOF detectors, and were accepted if they were within the range $0.14 < p_T < 1.2$ GeV/c in order to obtain good PID. The determination of the momenta of the tracks was performed using tracks reconstructed with the TPC only and constrained to the primary vertex. In order to reduce the number of secondary tracks (for instance the charged particles produced in the detector material, particles from weak decays, etc.), the primary charged kaon tracks were selected based on the DCA, such that the DCA transverse to the beam direction was less than 2.4 cm and the DCA along the beam direction was less than 3.2 cm. If the TOF signal were not available, the required N_σ values for the charged kaons were $N_\sigma^{\rm TPC} < 2$ for $p_T < 0.5$ GeV/c, and the track was rejected for $p_T > 0.5$ GeV/c. If the TOF signal were also available and $p_T > 0.5$ GeV/c: $N_\sigma^{\rm TPC} < 2$ and $N_\sigma^{\rm TOF} < 2$ ($0.5 < p_T < 1.2$ GeV/c).

The $K^0_S K^\pm$ experimental pair purity was estimated from a Monte Carlo (MC) study based on PYTHIA [17] simulations with the Perugia2011 tune [18], and using GEANT3 [19] to model particle transport through the ALICE detectors. The purity was determined from the fraction of the reconstructed MC simulated pairs that were identified as known $K^0_S K^\pm$ pairs from PYTHIA. The pair purity was estimated to be $\sim 83\%$ for all kinematic regions studied in this analysis. The single-particle purities for K^0_S and $K^\pm$ particles used in this analysis were estimated to be $\sim 92\%$ and $\sim 91\%$, respectively. The uncertainty in calculating the pair purity is estimated to be $\pm 1\%$.

3 Analysis methods

3.1 Experimental Correlation Functions

This analysis studies the momentum correlations of $K^0_S K^\pm$ pairs using the two-particle correlation function, defined as

$$C(k^*) = \frac{A(k^*)}{B(k^*)}, \tag{1}$$

where $A(k^*)$ is the measured distribution of pairs from the same event, $B(k^*)$ is the reference distribution of pairs from mixed events, and k^* is the magnitude of the momentum of each of the particles in the pair rest frame (PRF),

$$k^* = \sqrt{\frac{(s - m^2_{K^0} - m^2_{K^\pm})^2 - 4m^2_{K^0} m^2_{K^\pm}}{4s}} \tag{2}$$

where

$$s = m^2_{K^0} + m^2_{K^\pm} + 2E_{K^0}E_{K^\pm} - 2\vec{p}_{K^0} \cdot \vec{p}_{K^\pm} \tag{3}$$

and m_{K^0} (E_{K^0}) and $m_{K^\pm}$ ($E_{K^\pm}$) are the rest masses (total energies) of the K^0_S and $K^\pm$, respectively.

The denominator $B(k^*)$ was formed by mixing K^0_S and $K^\pm$ particles from each event with $K^\pm$ and K^0_S particles, respectively, from ten other events, where each event has at least both a $K^\pm$ and a K^0_S [2]. The vertices of the mixed events were constrained to be within 2 cm of each other in the z-direction.

Two-track effects, such as the merging of two real tracks into one reconstructed track and the splitting of one real track into two reconstructed tracks, is an important issue for femtoscopic studies. This analysis dealt with these effects using the following method. For each kaon pair, the distance between the K^0_S

pion daughter track and the same-charged $K^\pm$ track was calculated at up to nine points throughout the TPC (every 20 cm from 85 cm to 245 cm) and then averaged. Comparing pairs from the same event to those from mixed events, one observes a splitting peak for an average separation of < 11 cm. To correct for this, this analysis demanded that the same-charge particles from each kaon pair must have an average TPC separation of at least 13 cm. Mixed-event tracks were normalized by subtracting the primary vertex position from each used track point.

Correlation functions were created separately for the two different charge combinations, $K^0_S K^+$ and $K^0_S K^-$, and for three overlapping/non-exclusive pair transverse momentum $k_T = |\vec{p}_{T,1} + \vec{p}_{T,2}|/2$ ranges: all k_T, $k_T < 0.85$ and $k_T > 0.85$ GeV/c, where $k_T = 0.85$ GeV/c is the location of the peak of the k_T distribution. The mean k_T values for these three bins were 0.66, 0.49 and 1.17 GeV/c, respectively. The raw $K^0_S K^+$ correlation functions for these three bins compared with those generated from PYTHIA simulations with the Perugia2011 tune and using GEANT3 to model particle transport through the ALICE detectors are shown in Fig. 1. The PYTHIA correlation functions are normalized to the data in the vicinity of $k^* = 0.8$ GeV/c. The raw $K^0_S K^-$ correlation functions look very similar to these. It is seen that although PYTHIA qualitatively describes the trends of the baseline of the data, it does not describe it quantitatively such that it could be used to model the baseline directly. Instead, for the present analysis the strategy for dealing with the baseline was to describe it with several functional forms to be fitted to the experimental correlation functions and to use PYTHIA to test the appropriateness of the proposed baseline functional forms.

Three functional forms for the baseline were tested with PYTHIA: quadratic, Gaussian and exponential, given by

$$C_{\text{quadratic}}(k^*) = a(1 - bk^* + ck^{*2}) \tag{4}$$

$$C_{\text{Gaussian}}(k^*) = a(1 + b\exp(-ck^{*2})) \tag{5}$$

$$C_{\text{exponential}}(k^*) = a(1 + b\exp(-ck^*)) \tag{6}$$

where a, b and c are fit parameters. Fig. 2 shows fits of Eq. (4), Eq. (5) and Eq. (6) to the PYTHIA correlation functions shown in Fig. 1 for the three k_T ranges used in this analysis. As seen, all three functional forms do reasonably well in representing the PYTHIA correlation functions. Thus, all three forms were used in fitting the experimental correlation function and the different results obtained will be used to estimate the systematic uncertainty due to the baseline estimation. Of course there are an infinite number of functions one could try to represent the baseline, but at least the three that were chosen for this work are simple and representative of three basic functional forms.

Correlation functions were corrected for momentum resolution effects using PYTHIA calculations. The particle momentum resolution in ALICE for the relatively low-momentum tracks used in the present analysis was < 10 MeV/c [1]. Two correlation functions were generated with PYTHIA: one in terms of the generator-level k^* and one in terms of the simulated detector-level k^*. Because PYTHIA does not incorporate final-state interactions, simulated femtoscopic weights were determined using a 9th-order polynomial fit in k^* to the experimental correlation function for the k_T range considered. When filling the same-event distributions, i.e. $A(k^*)$ in Eq. 1, kaon pairs were individually weighted by this 9th-order fit according to their generator-level k^*. Then, the ratio of the "ideal" correlation function to the "measured" one (for each k^* bin) was multiplied to the data correlation functions before the fit procedure. This correction mostly affected the lowest k^* bins, increasing the extracted source parameters by $\sim 2\%$.

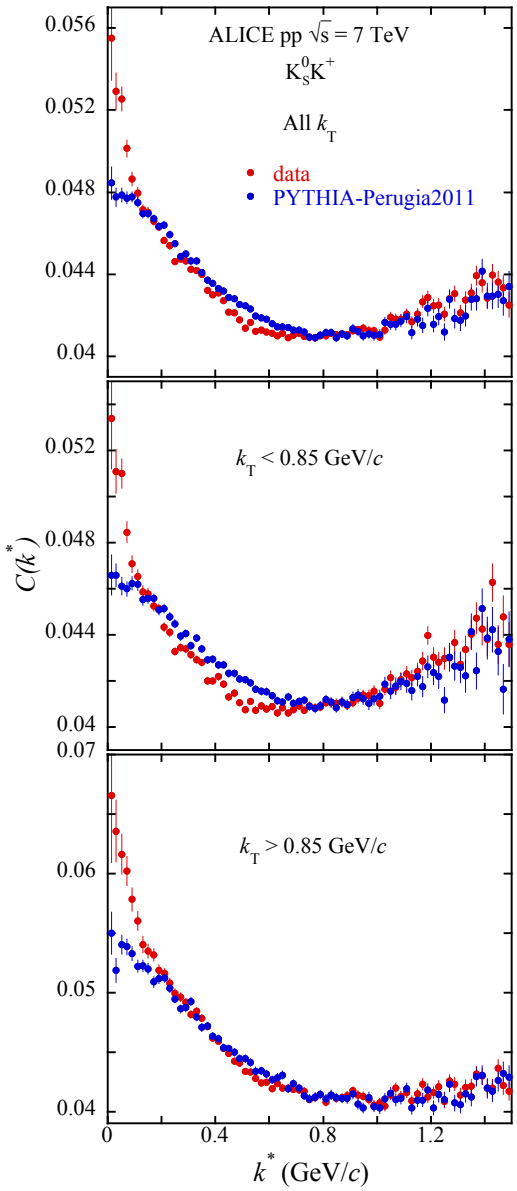

Figure 1: Raw $K^0_S K^+$ correlation functions for the three k_T bins compared with those from PYTHIA. The error bars are statistical. The scale of $C(k^*)$ is arbitrary. The PYTHIA correlation functions are normalized to the data in the vicinity of $k^* = 0.8$ GeV/c.

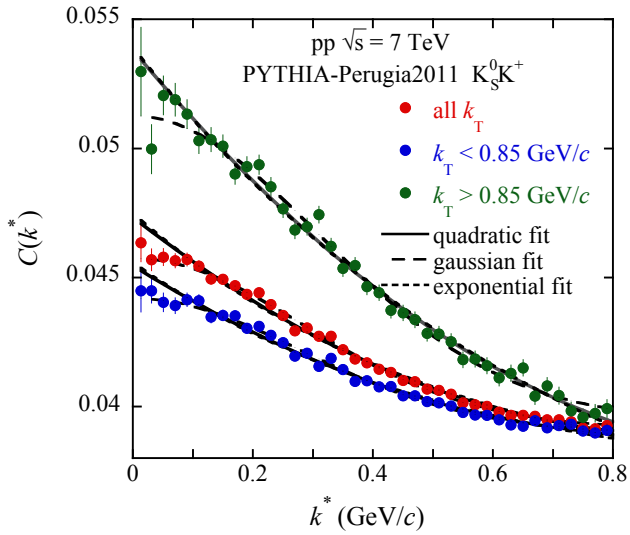

Figure 2: Comparisons of fits of three possible baseline functional forms with the PYTHIA correlation functions that were shown in Fig. 1. Fits were made in the k^* range $0-0.8$ GeV/c. The scale of $C(k^*)$ is arbitrary.

3.2 Final-state interaction model

The final-state interaction model used in the present pp collision analysis follows the same principles as the ones used for the ALICE Pb-Pb collision analysis [2]. The measured $K^0_S K^\pm$ correlation functions were fit with formulas that include a parameterization which incorporates strong FSI. It was assumed that the FSI arises in the $K^0_S K^\pm$ channels due to the near-threshold resonance, a_0. This parameterization was introduced by R. Lednicky and is based on the model by R. Lednicky and V.L. Lyuboshitz [20, 21] (see also Ref. [3] for more details on this parameterization).

Using an equal emission time approximation in the PRF [20], the elastic $K^0_S K^\pm$ transition is written as a stationary solution $\Psi_{-\vec{k}^*}(\vec{r}^*)$ of the scattering problem in the PRF. The quantity $\vec{r}^*$ represents the emission separation of the pair in the PRF, and the $-\vec{k}^*$ subscript refers to a reversal of time from the emission process. At large distances this has the asymptotic form of a superposition of an incoming plane wave and an outgoing spherical wave,

$$\Psi_{-\vec{k}^*}(\vec{r}^*) = e^{-i\vec{k}^*\cdot\vec{r}^*} + f(k^*)\frac{e^{ik^*r^*}}{r^*}\,, \tag{7}$$

where $f(k^*)$ is the s-wave K^0K^- or $\overline{K}^0K^+$ scattering amplitude whose contribution is the s-wave isovector a_0 resonance (see Eq. (11) in Ref. [3]) and

$$f(k^*) = \frac{\gamma_{a_0\to K\overline{K}}}{m^2_{a_0} - s - i(\gamma_{a_0\to K\overline{K}}k^* + \gamma_{a_0\to\pi\eta}k_{\pi\eta})}\,. \tag{8}$$

In Eq. (8), m_{a_0} is the mass of the a_0 resonance, and $\gamma_{a_0\to K\overline{K}}$ and $\gamma_{a_0\to\pi\eta}$ are the couplings of the a_0 resonance to the K^0K^- (or $\overline{K}^0K^+$) and $\pi\eta$ channels, respectively. Also, $s = 4(m^2_{K^0} + k^{*2})$ and $k_{\pi\eta}$ denotes the momentum in the second decay channel ($\pi\eta$) (see Tab. 1).

The correlation function due to the FSI is then calculated by integrating $\Psi_{-\vec{k}^*}(\vec{r}^*)$ in the *Koonin-Pratt equation* [22, 23],

$$C_{\rm FSI}(\vec{k}^*) = \int d^3\vec{r}^*\, S(\vec{r}^*)\left|\Psi_{-\vec{k}^*}(\vec{r}^*)\right|^2\,, \tag{9}$$

where $S(\vec{r}^*)$ is a one-dimensional Gaussian source function of the PRF relative distance $|\vec{r}^*|$ with a

Reference	m_{a_0}	$\gamma_{a_0\to K\overline{K}}$	$\gamma_{a_0\to\pi\eta}$
Achasov2 [7]	1.003	0.8365	0.4580

Table 1: The a_0 mass and coupling parameters, all in GeV/c^2, used in the present study.

Gaussian width R of the form

$$S(\vec{r}^*) \sim e^{-|\vec{r}^*|^2/(4R^2)}\,. \tag{10}$$

Equation 9 can be integrated analytically for $K^0_S K^\pm$ correlations with FSI for the one-dimensional case, with the result

$$C_{\rm FSI}(k^*) = 1 + \lambda\,\alpha\left[\frac{1}{2}\left|\frac{f(k^*)}{R}\right|^2 + \frac{2\mathscr{R}f(k^*)}{\sqrt{\pi}R}F_1(2k^*R) - \frac{\mathscr{I}f(k^*)}{R}F_2(2k^*R) + \Delta C\right], \tag{11}$$

where

$$F_1(z) \equiv \frac{\sqrt{\pi}e^{-z^2}\,\mathrm{erfi}(z)}{2z}; \qquad F_2(z) \equiv \frac{1-e^{-z^2}}{z}. \tag{12}$$

In the above equations α is the fraction of $K^0_S K^\pm$ pairs that come from the K^0K^- or $\overline{K}^0K^+$ system, set to 0.5 assuming symmetry in K^0 and $\overline{K}^0$ production [3], R is the radius parameter from the spherical Gaussian source distribution given in Eq. (10), and λ is the correlation strength. The correlation strength is unity in the ideal case of pure a_0-resonant FSI, perfect PID, a perfect Gaussian kaon source and the absence of long-lived resonances which decay into kaons. The term ΔC is a calculated correction factor that takes into account the deviation of the spherical wave assumption used in Eq. (7) in the inner region of the short-range potential (see the Appendix in Ref. [3]). Its effect on the extracted R and λ parameters is to increase them by $\sim 14\%$. Note that the form of the FSI term in Eq. (11) differs from the form of the FSI term for $K^0_S K^0_S$ correlations (Eq. (9) of Ref. [3]) by a factor of $1/2$ due to the non-identical particles in $K^0_S K^\pm$ correlations and thus the absence of the requirement to symmetrize the wavefunction given in Eq. (7).

As seen in Eq. (8), the K^0K^- or $\overline{K}^0K^+$ s-wave scattering amplitude depends on the a_0 mass and decay couplings. From the ALICE Pb-Pb collision $K^0_S K^\pm$ study [2], it was found that source parameters extracted with the "Achasov2" parameters of Ref. [7] agreed best with the identical kaon measurements, thus in the present pp collision study only the Achasov2 parameters are used. These parameters are shown in Tab. 1. Since the correction factor ΔC is found to mainly depend on $\gamma_{a_0K\bar{K}}$ [3], it is judged that the systematic uncertainty on the calculation of ΔC is negligible.

The experimental $K^0_S K^\pm$ correlation functions, calculated using Eq. (1), were fit with the expression

$$C(k^*) = C_{\rm FSI}(k^*)C_{\rm baseline}(k^*), \tag{13}$$

where $C_{\rm baseline}(k^*)$ is Eq. (4), Eq. (5) or Eq. (6).

The fitting strategy used was to carry out a 5-parameter fit of Eq. (13) to the $K^0_S K^\pm$ experimental correlation functions to extract R, λ, a, b and c for each of the six (k_T range)-(charge state) combinations. For each of these six combinations, the three baseline functional forms, and two k^* fit ranges, (0.0-0.6 GeV/c) and (0.0-0.8 GeV/c), were fit, giving six R and six λ parameter values for each combination. These six values were then averaged and the variance calculated to obtain the final values for the parameters and an estimate of the combined systematic uncertainties from the baseline assumptions and fit range, respectively.

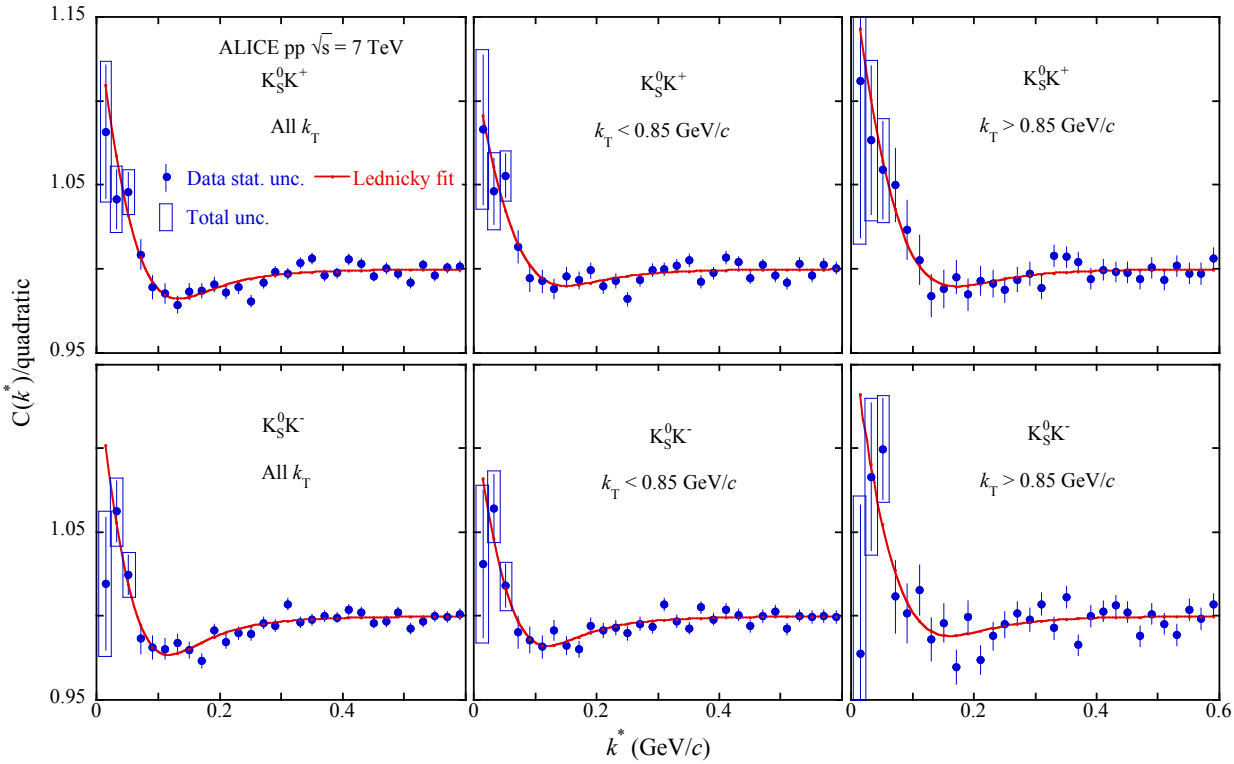

Figure 3: Correlation functions divided by one of the baseline functions with fits from Eq. (13) for $K^0_S K^+$ and $K^0_S K^-$ and k^* fit range (0.0-0.6 GeV/c) for the three k_T bins and the quadratic baseline function assumption. Statistical (lines) and the quadratic sum of the statistical and systematic (boxes) uncertainties are shown. For $k^* > 0.05$ GeV/c, the systematic uncertainties become negligible and the boxes are no longer shown.

4 Results and discussion

4.1 Fits to the experimental correlation functions

Figure 3 shows sample correlation functions divided by the quadratic baseline function with fits of Eq. (13) for $K^0_S K^\pm$ and the k^* fit range ($0.0-0.6$ GeV/c) for the three k_T bins. The fits using the other baseline assumptions and to the wider range of ($0.0-0.8$ GeV/c) are similar in quality. Comparing with the quadratic baseline, using the Gaussian baseline tends to give $\sim 10-20\%$ smaller source parameters whereas using the exponential baseline tends to give $\sim 10-20\%$ larger source parameters. The average χ^2/ndf and p-value over all of the fits are 1.554 and 0.172, respectively. Statistical (lines) and the quadratic sum of the statistical and systematic (boxes) uncertainties are shown. The systematic uncertainties were determined by varying cuts on the data (See the discussion of the "cut systematic uncertainty" in the section below on "Systematic Uncertainties for more details."). Fig. 4 shows sample raw correlation functions for $K^0_S K^+$ for the three k_T bins and the quadratic baseline function, Eq. 4, that was fit corresponding to the 5-parameter fits of Eq. 13 to the $K^0_S K^+$ data presented in Fig. 3. Statistical uncertainties on the fit parameters were obtained by constructing the 1σ λ vs. R contour and taking the errors to be at the extreme extents of the contour. A typical value of the correlation coefficient is 0.642. This method gives the most conservative estimates of the statistical uncertainties.

The Achasov2 a_0 FSI parameterization coupled with the various baseline assumptions gives a good representation of the signal region of the data, i.e. reproducing the enhancement in the k^* region $0.0-0.1$ GeV/c and the small dip in the region $0.1-0.3$ GeV/c. A good representation of the signal region was also seen to be the case for the Pb-Pb analysis with the Achasov2 parameterization, which has a qualitatively different k^* dependence of the correlation function that is dominated by a dip at low k^* (Compare present Fig. 3 with Fig. 2 from Ref. [2]). The enhancement seen for the small-R system at low

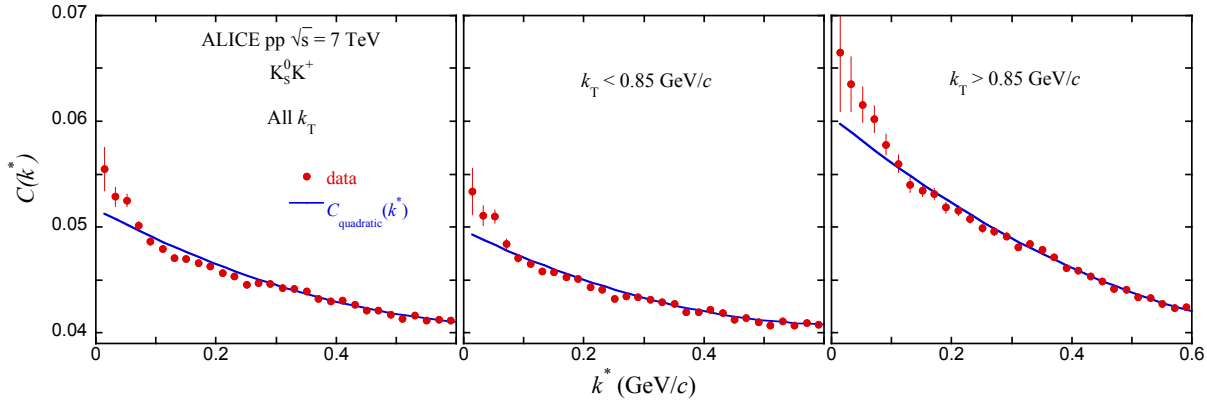

Figure 4: Sample raw correlation functions for $K^0_S K^+$ showing the fitted quadratic baseline function, Eq. 4. Statistical uncertainties are shown. The scale of $C(k^*)$ is arbitrary.

R or λ [+/-]	k_T cut (GeV/c)	fit value	statistical uncert.	fit systematic uncert.	cut systematic uncert.	total systematic uncert.	total quadratic uncert.
R[+] (fm)	$k_T < 0.85$	0.905	0.063	0.243	0.033	0.245	0.253
	$k_T > 0.85$	0.788	0.077	0.168	0.031	0.171	0.188
	All k_T	0.922	0.048	0.188	0.038	0.192	0.198
λ[+]	$k_T < 0.85$	0.189	0.046	0.070	0.012	0.071	0.085
	$k_T > 0.85$	0.222	0.080	0.066	0.015	0.068	0.105
	All k_T	0.242	0.046	0.066	0.020	0.069	0.083
R[-] (fm)	$k_T < 0.85$	1.039	0.060	0.244	0.039	0.247	0.254
	$k_T > 0.85$	0.786	0.082	0.145	0.032	0.148	0.169
	All k_T	0.995	0.046	0.185	0.041	0.190	0.195
λ[-]	$k_T < 0.85$	0.253	0.044	0.096	0.016	0.097	0.107
	$k_T > 0.85$	0.208	0.084	0.038	0.016	0.042	0.094
	All k_T	0.277	0.038	0.074	0.023	0.078	0.087

Table 2: Fit results for average R and λ showing statistical and systematic uncertainties from $K^0_S K^\pm$ femtoscopy with pp collisions at $\sqrt{s} = 7$ TeV. The "[+/-]" in the first column refers to $K^0_S K^+$ or $K^0_S K^-$. See the text for the definitions of the various uncertainties.

k^* is expected from Eq. (11) as a consequence of the first term in the brackets that goes as $1/R^2$. This demonstrates the ability of Eq. (11) to describe the FSI in both the small and large size regimes as going through the a_0 resonance.

4.2 Extracted R and λ parameters

The results for the extracted average R and λ parameters and the statistical and systematic uncertainties on these for the present analysis of $K^0_S K^\pm$ femtoscopy from 7 TeV pp collisions are shown in Tab. 2. The statistical uncertainties given are the averages over the 6 fits for each case. As can be seen, R and λ for $K^0_S K^+$ agree within the statistical uncertainties with those for $K^0_S K^-$ in all cases.

4.3 Systematic uncertainties

Table 2 shows the total systematic uncertainties on the extracted R and λ parameters. As is seen, for most cases the total systematic uncertainty is larger than the statistical uncertainty. The total systematic uncertainty is broken down in Tab. 2 into two main contributions, the "fit systematic uncertainty" and the "cut systematic uncertainty", and is the quadratic sum of these. The fit systematic uncertainty is the combined systematic uncertainty due to the various baseline assumptions and varying the k^* fit range,

as described earlier. The cut systematic uncertainty is the systematic uncertainty related to the various cuts made in the data analysis. To determine this, single particle cuts were varied by $\sim 10\%$, and the value chosen for the minimum separation distance of same-sign tracks was varied by $\sim 20\%$. Taking the upper-limit values of the variations to be conservative, this led to additional errors of 4% for R and 8% for λ. As seen in the table, the fit systematic uncertainty dominates over the cut systematic uncertainty in all cases, demonstrating the large uncertainties in determining the non-femtoscopic baseline in pp collisions. The "total quadratic uncertainty" is the quadratic sum of the "statistical uncertainty" column and the "total systematic uncertainty" column.

4.4 Comparisons with $K^0_S K^\pm$ results from Pb-Pb collisions at $\sqrt{s_{NN}} = 2.76$ TeV and identical-kaon results from pp collisions at $\sqrt{s} = 7$ TeV

In this section comparisons of the present results for R and λ with $K^0_S K^\pm$ measurements from ALICE 2.76 TeV Pb-Pb collisions for $0-10\%$ centrality [2], and with identical-kaon measurements from ALICE 7 TeV pp collisions [4, 5] are presented. Since it is seen in Tab. 2 that the extracted parameters for $K^0_S K^+$ agree within the statistical uncertainties with those for $K^0_S K^-$ in all cases, these are averaged over weighted by the statistical uncertainties in the following figures

Figure 5 shows the comparison with the ALICE Pb-Pb collision $K^0_S K^\pm$ measurements. The λ parameters have been divided by the pair purity for each case, i.e. 83% for the present pp collisions and 88% for the Pb-Pb collisions [2], so that they can be compared on the same basis. It is seen that R for $0-10\%$ centrality Pb-Pb is ~ 5 fm, and is significantly larger than the $R \sim 1$ fm measured for pp collisions. This is expected since R reflects the geometric size of the interaction region of the collision. It is somewhat surprising that λ for pp collisions is seen to be significantly less than that for Pb-Pb collisions. There are two main factors effecting the value of the λ parameter: 1) the degree to which a Gaussian fits the correlation function and 2) the effect of long-lived resonances diluting the kaon sample. For 1), it is seen in Fig. 3 for pp and in Fig. 2 of Ref. [2] for Pb-Pb that the Gaussian function used in the Ledincky equation, Eqs. 10 and 11, fits both colliding systems well, minimizing the effect of 1). For 2), the K^* decay ($\Gamma \sim 50$ MeV) has the largest influence on diluting the kaon sample, and it is unlikely that the multiplicity ratio of K/K^* changes dramatically in going from 2.76 TeV to 7 TeV. From these arguments we might naively expect λ to be similar in the pp and Pb-Pb cases.

In order to properly compare the present results with the ALICE pp collision identical-kaon measurements, we must take the weighted average (weighted by their statistical uncertainties) over the multiplicity bins used in Refs. [4, 5] since our present results are summed over all multiplicity. Figure 6 shows the comparison between the present results for R and λ and measurements from the identical-kaon femtoscopy in 7 TeV pp collisions. The R values are seen to agree between the present analysis and the identical kaon analyses within the uncertainties. The λ parameters shown in Fig. 6 are each divided by their respective pair purities. Going from the lowest to the highest k_T points, for the neutral-kaon pairs the purities are 0.88 and 0.84 [4], and for the charge-kaon pairs the purities are 0.84, 0.61, 0.79 and 1.0 [5], respectively. The purity-normalized λ parameters for the identical kaons are seen to scatter in a wide range between values of $0.3-0.7$, whereas the $K^0_S K^\pm$ values are seen to lie in the narrower range of $0.25-0.30$.

In order to help to clarify the comparison between the purity-normalized λ values from $K^0_S K^\pm$ and the identical-kaon results, the simple average over the identical kaon purity-normalized λ parameters is plotted as a blue dashed line in Fig. 6. As seen, the $K^0_S K^\pm$ values tend to be smaller than the average of the identical kaons, as was more significantly the case for the comparison with the purity-normalized λ values from Pb-Pb seen in Fig. 5, however the large scatter of the identical kaons makes it difficult to draw any strong conclusions from this comparison.

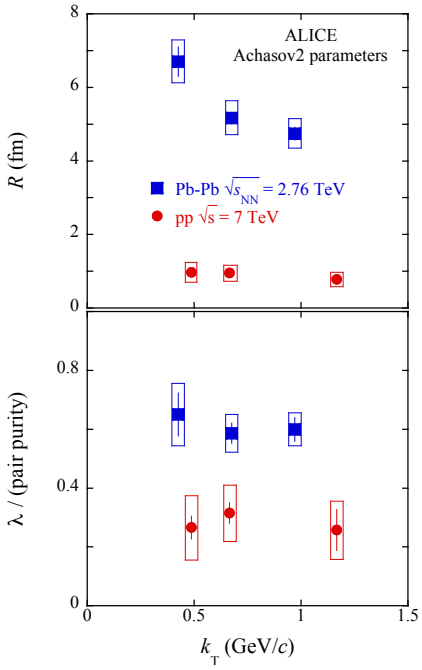

Figure 5: R and λ parameters extracted in the present analysis from $K^0_S K^\pm$ femtoscopy averaged over $K^0_S K^+$ and $K^0_S K^-$, along with a comparison with $K^0_S K^\pm$ results from ALICE 2.76 TeV Pb-Pb collisions for $0-10\%$ centrality [2]. The quadratic sum of the statistical and systematic uncertainties is plotted for all results as boxes and the statistical uncertainties are given as lines. The λ parameters have been divided by their respective pair purities to facilitate their comparison.

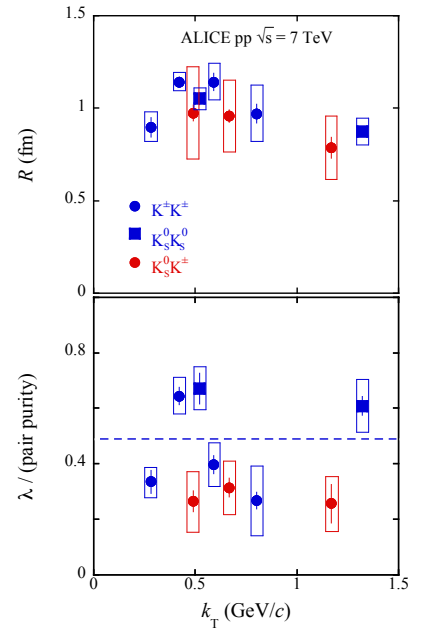

Figure 6: R and purity-normalized λ parameters extracted in the present analysis from $K^0_S K^\pm$ femtoscopy averaged over $K^0_S K^+$ and $K^0_S K^-$, along with comparisons with identical kaon results from ALICE 7 TeV pp collisions averaged over event multiplicity. The quadratic sum of the statistical and systematic uncertainties is plotted for all results as boxes and the statistical uncertainties are given as lines. Also plotted as a blue dashed line is the simple average of the identical-kaon purity-normalized λ parameters.

4.5 Implications from the present results for the a_0 to be a tetraquark state

The $K^0_S K^\pm$ FSI is described well by assuming it is due to the a_0 resonance for both pp and Pb-Pb collisions, as seen in Fig. 3 of the present work and in Fig. 2 of Ref. [2]. The *R* parameters extracted from this method are also seen to agree within uncertainties with the identical-kaon measurements for each of these collision systems. For Pb-Pb collisions, it was found that the λ parameters extracted from $K^0_S K^\pm$ also agree with the corresponding identical-kaon measurements for Pb-Pb collisions indicating that the FSI between the kaons goes solely through the a_0 resonance. The present pp collision results for λ, which are significantly lower than the $K^0_S K^\pm$ values from Pb-Pb collisions seen in Fig. 5 and which tend to be lower than the corresponding identical-kaon values in pp collisions seen in Fig. 6, imply that the FSI for these collisions does not go solely through the a_0 resonance, i.e. non-resonant elastic channels and/or free-streaming are also present. From the arguments given in the Introduction, this is the geometric effect that would be expected in the case of a tetraquark a_0 since competing annihilation channels could open up in the smaller system and compete with the FSI through the a_0, whereas for a diquark a_0 the FSI should still go solely through the a_0. The pp collision results are thus compatible with the conclusion from the Pb-Pb collision measurement [2] that favors the interpretation of the a_0 resonance to be a tetraquark state.

5 Summary

In summary, femtoscopic correlations with the particle pair combinations $K^0_S K^\pm$ are studied in pp collisions at $\sqrt{s} = 7$ TeV for the first time by the LHC ALICE experiment. Correlations in the $K^0_S K^\pm$ pairs are produced by final-state interactions which proceed through the a_0 resonance. It is found that the a_0 final-state interaction describes the shape of the measured $K^0_S K^\pm$ correlation functions well. The extracted radius and λ parameters for $K^0_S K^-$ are found to be equal within the experimental uncertainties to those for $K^0_S K^+$. Results of the present study are compared with those from identical-kaon femtoscopic studies also performed with pp collisions at $\sqrt{s} = 7$ TeV by ALICE and with a recent ALICE $K^0_S K^\pm$ measurement in Pb-Pb collisions at $\sqrt{s_{\rm NN}} = 2.76$ TeV. These comparisons suggest that non-resonant elastic scattering channels are present in pp collisions, unlike in Pb-Pb collisions. It is our conclusion that the present results, in combination with the ALICE Pb-Pb collision measurements, favor the interpretation of the a_0 to be a tetraquark state.

Acknowledgements

The ALICE Collaboration would like to thank all its engineers and technicians for their invaluable contributions to the construction of the experiment and the CERN accelerator teams for the outstanding performance of the LHC complex. The ALICE Collaboration gratefully acknowledges the resources and support provided by all Grid centres and the Worldwide LHC Computing Grid (WLCG) collaboration. The ALICE Collaboration acknowledges the following funding agencies for their support in building and running the ALICE detector: A. I. Alikhanyan National Science Laboratory (Yerevan Physics Institute) Foundation (ANSL), State Committee of Science and World Federation of Scientists (WFS), Armenia; Austrian Academy of Sciences and Nationalstiftung für Forschung, Technologie und Entwicklung, Austria; Ministry of Communications and High Technologies, National Nuclear Research Center, Azerbaijan; Conselho Nacional de Desenvolvimento Científico e Tecnológico (CNPq), Universidade Federal do Rio Grande do Sul (UFRGS), Financiadora de Estudos e Projetos (Finep) and Fundação de Amparo à Pesquisa do Estado de São Paulo (FAPESP), Brazil; Ministry of Science & Technology of China (MSTC), National Natural Science Foundation of China (NSFC) and Ministry of Education of China (MOEC) , China; Ministry of Science and Education, Croatia; Centro de Aplicaciones Tecnológicas y Desarrollo Nuclear (CEADEN), Cubaenergía, Cuba; Ministry of Education, Youth and Sports of the Czech Republic, Czech Republic; The Danish Council for Independent Research — Natural Sciences,

the Carlsberg Foundation and Danish National Research Foundation (DNRF), Denmark; Helsinki Institute of Physics (HIP), Finland; Commissariat à l'Energie Atomique (CEA) and Institut National de Physique Nucléaire et de Physique des Particules (IN2P3) and Centre National de la Recherche Scientifique (CNRS), France; Bundesministerium für Bildung, Wissenschaft, Forschung und Technologie (BMBF) and GSI Helmholtzzentrum für Schwerionenforschung GmbH, Germany; General Secretariat for Research and Technology, Ministry of Education, Research and Religions, Greece; National Research, Development and Innovation Office, Hungary; Department of Atomic Energy Government of India (DAE), Department of Science and Technology, Government of India (DST), University Grants Commission, Government of India (UGC) and Council of Scientific and Industrial Research (CSIR), India; Indonesian Institute of Science, Indonesia; Centro Fermi - Museo Storico della Fisica e Centro Studi e Ricerche Enrico Fermi and Istituto Nazionale di Fisica Nucleare (INFN), Italy; Institute for Innovative Science and Technology , Nagasaki Institute of Applied Science (IIST), Japan Society for the Promotion of Science (JSPS) KAKENHI and Japanese Ministry of Education, Culture, Sports, Science and Technology (MEXT), Japan; Consejo Nacional de Ciencia (CONACYT) y Tecnología, through Fondo de Cooperación Internacional en Ciencia y Tecnología (FONCICYT) and Dirección General de Asuntos del Personal Academico (DGAPA), Mexico; Nederlandse Organisatie voor Wetenschappelijk Onderzoek (NWO), Netherlands; The Research Council of Norway, Norway; Commission on Science and Technology for Sustainable Development in the South (COMSATS), Pakistan; Pontificia Universidad Católica del Perú, Peru; Ministry of Science and Higher Education and National Science Centre, Poland; Korea Institute of Science and Technology Information and National Research Foundation of Korea (NRF), Republic of Korea; Ministry of Education and Scientific Research, Institute of Atomic Physics and Romanian National Agency for Science, Technology and Innovation, Romania; Joint Institute for Nuclear Research (JINR), Ministry of Education and Science of the Russian Federation and National Research Centre Kurchatov Institute, Russia; Ministry of Education, Science, Research and Sport of the Slovak Republic, Slovakia; National Research Foundation of South Africa, South Africa; Swedish Research Council (VR) and Knut & Alice Wallenberg Foundation (KAW), Sweden; European Organization for Nuclear Research, Switzerland; National Science and Technology Development Agency (NSDTA), Suranaree University of Technology (SUT) and Office of the Higher Education Commission under NRU project of Thailand, Thailand; Turkish Atomic Energy Agency (TAEK), Turkey; National Academy of Sciences of Ukraine, Ukraine; Science and Technology Facilities Council (STFC), United Kingdom; National Science Foundation of the United States of America (NSF) and United States Department of Energy, Office of Nuclear Physics (DOE NP), United States of America.

References

[1] **ALICE** Collaboration, K. Aamodt *et al.*, "The ALICE experiment at the CERN LHC," *JINST* **3** (2008) S08002.

[2] **ALICE** Collaboration, S. Acharya *et al.*, "Measuring $K^0_S K^\pm$ interactions using Pb-Pb collisions at $\sqrt{s_{\rm NN}} = 2.76$ TeV," *Phys. Lett.* **B774** (2017) 64–77, arXiv:1705.04929 [nucl-ex].

[3] **STAR** Collaboration, B. I. Abelev *et al.*, "Neutral kaon interferometry in Au+Au collisions at $\sqrt{s_{NN}} = 200$ GeV," *Phys. Rev.* **C74** (2006) 054902, arXiv:nucl-ex/0608012 [nucl-ex].

[4] **ALICE** Collaboration, B. Abelev *et al.*, "$K^0_s - K^0_s$ correlations in pp collisions at $\sqrt{s} = 7$ TeV from the LHC ALICE experiment," *Phys. Lett.* **B717** (2012) 151–161, arXiv:1206.2056 [hep-ex].

[5] **ALICE** Collaboration, B. Abelev *et al.*, "Charged kaon femtoscopic correlations in *pp* collisions at $\sqrt{s} = 7$ TeV," *Phys. Rev.* **D87** no. 5, (2013) 052016, arXiv:1212.5958 [hep-ex].

[6] **ALICE** Collaboration, J. Adam *et al.*, "One-dimensional pion, kaon, and proton femtoscopy in Pb-Pb collisions at $\sqrt{s_{\rm NN}} = 2.76$ TeV," *Phys. Rev.* **C92** no. 5, (2015) 054908, arXiv:1506.07884 [nucl-ex].

[7] N. N. Achasov and A. V. Kiselev, "The New analysis of the KLOE data on the $\phi \to \eta\pi^0\gamma$ decay," *Phys. Rev.* **D68** (2003) 014006, arXiv:hep-ph/0212153 [hep-ph].

[8] E. Santopinto and G. Galata, "Spectroscopy of tetraquark states," *Phys. Rev.* **C75** (2007) 045206, arXiv:hep-ph/0605333 [hep-ph].

[9] R. L. Jaffe, "Multi-Quark Hadrons. 1. The Phenomenology of $qq\overline{qq}$ Mesons," *Phys. Rev.* **D15** (1977) 267.

[10] N. N. Achasov and A. V. Kiselev, "Light scalar mesons and two-kaon correlation functions," *Phys. Rev.* **D97** no. 3, (2018) 036015, arXiv:1711.08777 [hep-ph].

[11] **ALICE** Collaboration, B. B. Abelev *et al.*, "Performance of the ALICE Experiment at the CERN LHC," *Int. J. Mod. Phys.* **A29** (2014) 1430044, arXiv:1402.4476 [nucl-ex].

[12] A. Akindinov *et al.*, "Performance of the ALICE Time-Of-Flight detector at the LHC," *Eur. Phys. J. Plus* **128** (2013) 44.

[13] **ALICE** Collaboration, B. Abelev *et al.*, "Centrality dependence of π, K, p production in Pb-Pb collisions at $\sqrt{s_{NN}} = 2.76$ TeV," *Phys. Rev.* **C88** (2013) 044910, arXiv:1303.0737 [hep-ex].

[14] **ALICE** Collaboration, B. Abelev *et al.*, "Centrality determination of Pb-Pb collisions at $\sqrt{s_{\rm NN}}$=2.76 TeV with ALICE," *Phys. Rev.* **C88** no. 4, (2013) 044909, arXiv:1301.4361 [nucl-ex].

[15] J. Alme *et al.*, "The ALICE TPC, a large 3-dimensional tracking device with fast readout for ultra-high multiplicity events," *Nucl. Instrum. Meth.* **A622** (2010) 316–367, arXiv:1001.1950 [physics.ins-det].

[16] **ALICE** Collaboration, B. Alessandro *et al.*, "ALICE: Physics performance report, volume II," *J. Phys.* **G32** (2006) 1295–2040.

[17] T. Sjostrand, S. Mrenna, and P. Skands, "PYTHIA 6.4 Physics and Manual," *JHEP* **05** (2006) 026, arXiv:hep-ph/0603175.

[18] P. Z. Skands, "Tuning Monte Carlo Generators: The Perugia Tunes," *Phys. Rev.* **D82** (2010) 074018, arXiv:1005.3457 [hep-ph].

[19] R. Brun, F. Bruyant, F. Carminati, S. Giani, M. Maire, A. McPherson, G. Patrick, and L. Urban, "GEANT Detector Description and Simulation Tool," *CERN-W5013* **1** (1994) 1.

[20] R. Lednicky and V. Lyuboshits, "Final State Interaction Effect on Pairing Correlations Between Particles with Small Relative Momenta," *Sov. J. Nucl. Phys.* **35** (1982) 770.

[21] R. Lednicky, "Correlation femtoscopy," *Nucl. Phys.* **A774** (2006) 189–198, arXiv:nucl-th/0510020 [nucl-th].

[22] S. Koonin, "Proton Pictures of High-Energy Nuclear Collisions," *Phys. Lett.* **B70** (1977) 43–47.

[23] S. Pratt, T. Csorgo, and J. Zimanyi, "Detailed predictions for two pion correlations in ultrarelativistic heavy ion collisions," *Phys. Rev.* **C42** (1990) 2646–2652.

A The ALICE Collaboration

S. Acharya[139], F.T.-. Acosta[20], D. Adamová[93], A. Adler[74], J. Adolfsson[80], M.M. Aggarwal[98], G. Aglieri Rinella[34], M. Agnello[31], N. Agrawal[48], Z. Ahammed[139], S.U. Ahn[76], S. Aiola[144], A. Akindinov[64], M. Al-Turany[104], S.N. Alam[139], D.S.D. Albuquerque[121], D. Aleksandrov[87], B. Alessandro[58], H.M. Alfanda[6], R. Alfaro Molina[72], Y. Ali[15], A. Alici[10,27,53], A. Alkin[2], J. Alme[22], T. Alt[69], L. Altenkamper[22], I. Altsybeev[111], M.N. Anaam[6], C. Andrei[47], D. Andreou[34], H.A. Andrews[108], A. Andronic[104,142], M. Angeletti[34], V. Anguelov[102], C. Anson[16], T. Antičić[105], F. Antinori[56], P. Antonioli[53], R. Anwar[125], N. Apadula[79], L. Aphecetche[113], H. Appelshäuser[69], S. Arcelli[27], R. Arnaldi[58], M. Arratia[79], I.C. Arsene[21], M. Arslandok[102], A. Augustinus[34], R. Averbeck[104], M.D. Azmi[17], A. Badalà[55], Y.W. Baek[40,60], S. Bagnasco[58], R. Bailhache[69], R. Bala[99], A. Baldisseri[135], M. Ball[42], R.C. Baral[85], A.M. Barbano[26], R. Barbera[28], F. Barile[52], L. Barioglio[26], G.G. Barnaföldi[143], L.S. Barnby[92], V. Barret[132], P. Bartalini[6], K. Barth[34], E. Bartsch[69], N. Bastid[132], S. Basu[141], G. Batigne[113], B. Batyunya[75], P.C. Batzing[21], J.L. Bazo Alba[109], I.G. Bearden[88], H. Beck[102], C. Bedda[63], N.K. Behera[60], I. Belikov[134], F. Bellini[34], H. Bello Martinez[44], R. Bellwied[125], L.G.E. Beltran[119], V. Belyaev[91], G. Bencedi[143], S. Beole[26], A. Bercuci[47], Y. Berdnikov[96], D. Berenyi[143], R.A. Bertens[128], D. Berzano[34,58], L. Betev[34], P.P. Bhaduri[139], A. Bhasin[99], I.R. Bhat[99], H. Bhatt[48], B. Bhattacharjee[41], J. Bhom[117], A. Bianchi[26], L. Bianchi[26,125], N. Bianchi[51], J. Bielčík[37], J. Bielčíková[93], A. Bilandzic[103,116], G. Biro[143], R. Biswas[3], S. Biswas[3], J.T. Blair[118], D. Blau[87], C. Blume[69], G. Boca[137], F. Bock[34], A. Bogdanov[91], L. Boldizsár[143], A. Bolozdynya[91], M. Bombara[38], G. Bonomi[138], M. Bonora[34], H. Borel[135], A. Borissov[102,142], M. Borri[127], E. Botta[26], C. Bourjau[88], L. Bratrud[69], P. Braun-Munzinger[104], M. Bregant[120], T.A. Broker[69], M. Broz[37], E.J. Brucken[43], E. Bruna[58], G.E. Bruno[33,34], D. Budnikov[106], H. Buesching[69], S. Bufalino[31], P. Buhler[112], P. Buncic[34], O. Busch[I,131], Z. Buthelezi[73], J.B. Butt[15], J.T. Buxton[95], J. Cabala[115], D. Caffarri[89], H. Caines[144], A. Caliva[104], E. Calvo Villar[109], R.S. Camacho[44], P. Camerini[25], A.A. Capon[112], W. Carena[34], F. Carnesecchi[10,27], J. Castillo Castellanos[135], A.J. Castro[128], E.A.R. Casula[54], C. Ceballos Sanchez[8], S. Chandra[139], B. Chang[126], W. Chang[6], S. Chapeland[34], M. Chartier[127], S. Chattopadhyay[139], S. Chattopadhyay[107], A. Chauvin[24], C. Cheshkov[133], B. Cheynis[133], V. Chibante Barroso[34], D.D. Chinellato[121], S. Cho[60], P. Chochula[34], T. Chowdhury[132], P. Christakoglou[89], C.H. Christensen[88], P. Christiansen[80], T. Chujo[131], S.U. Chung[18], C. Cicalo[54], L. Cifarelli[10,27], F. Cindolo[53], J. Cleymans[124], F. Colamaria[52], D. Colella[52], A. Collu[79], M. Colocci[27], M. Concas[II,58], G. Conesa Balbastre[78], Z. Conesa del Valle[61], J.G. Contreras[37], T.M. Cormier[94], Y. Corrales Morales[58], P. Cortese[32], M.R. Cosentino[122], F. Costa[34], S. Costanza[137], J. Crkovská[61], P. Crochet[132], E. Cuautle[70], L. Cunqueiro[94,142], D. Dabrowski[140], T. Dahms[103,116], A. Dainese[56], F.P.A. Damas[113,135], S. Dani[66], M.C. Danisch[102], A. Danu[68], D. Das[107], I. Das[107], S. Das[3], A. Dash[85], S. Dash[48], S. De[49], A. De Caro[30], G. de Cataldo[52], C. de Conti[120], J. de Cuveland[39], A. De Falco[24], D. De Gruttola[10,30], N. De Marco[58], S. De Pasquale[30], R.D. De Souza[121], H.F. Degenhardt[120], A. Deisting[102,104], A. Deloff[84], S. Delsanto[26], C. Deplano[89], P. Dhankher[48], D. Di Bari[33], A. Di Mauro[34], B. Di Ruzza[56], R.A. Diaz[8], T. Dietel[124], P. Dillenseger[69], Y. Ding[6], R. Divià[34], Ø. Djuvsland[22], A. Dobrin[34], D. Domenicis Gimenez[120], B. Dönigus[69], O. Dordic[21], A.K. Dubey[139], A. Dubla[104], L. Ducroux[133], S. Dudi[98], A.K. Duggal[98], M. Dukhishyam[85], P. Dupieux[132], R.J. Ehlers[144], D. Elia[52], E. Endress[109], H. Engel[74], E. Epple[144], B. Erazmus[113], F. Erhardt[97], A. Erokhin[111], M.R. Ersdal[22], B. Espagnon[61], G. Eulisse[34], J. Eum[18], D. Evans[108], S. Evdokimov[90], L. Fabbietti[103,116], M. Faggin[29], J. Faivre[78], A. Fantoni[51], M. Fasel[94], L. Feldkamp[142], A. Feliciello[58], G. Feofilov[111], A. Fernández Téllez[44], A. Ferretti[26], A. Festanti[34], V.J.G. Feuillard[102], J. Figiel[117], M.A.S. Figueredo[120], S. Filchagin[106], D. Finogeev[62], F.M. Fionda[22], G. Fiorenza[52], F. Flor[125], M. Floris[34], S. Foertsch[73], P. Foka[104], S. Fokin[87], E. Fragiacomo[59], A. Francescon[34], A. Francisco[113], U. Frankenfeld[104], G.G. Fronze[26], U. Fuchs[34], C. Furget[78], A. Furs[62], M. Fusco Girard[30], J.J. Gaardhøje[88], M. Gagliardi[26], A.M. Gago[109], K. Gajdosova[88], M. Gallio[26], C.D. Galvan[119], P. Ganoti[83], C. Garabatos[104], E. Garcia-Solis[11], K. Garg[28], C. Gargiulo[34], K. Garner[142], P. Gasik[103,116], E.F. Gauger[118], M.B. Gay Ducati[71], M. Germain[113], J. Ghosh[107], P. Ghosh[139], S.K. Ghosh[3], P. Gianotti[51], P. Giubellino[58,104], P. Giubilato[29], P. Glässel[102], D.M. Goméz Coral[72], A. Gomez Ramirez[74], V. Gonzalez[104], P. González-Zamora[44], S. Gorbunov[39], L. Görlich[117], S. Gotovac[35], V. Grabski[72], L.K. Graczykowski[140], K.L. Graham[108], L. Greiner[79], A. Grelli[63], C. Grigoras[34], V. Grigoriev[91], A. Grigoryan[1], S. Grigoryan[75], J.M. Gronefeld[104], F. Grosa[31], J.F. Grosse-Oetringhaus[34], R. Grosso[104], R. Guernane[78], B. Guerzoni[27], M. Guittiere[113], K. Gulbrandsen[88], T. Gunji[130], A. Gupta[99], R. Gupta[99], I.B. Guzman[44], R. Haake[34,144], M.K. Habib[104], C. Hadjidakis[61], H. Hamagaki[81], G. Hamar[143], M. Hamid[6], J.C. Hamon[134], R. Hannigan[118], M.R. Haque[63], A. Harlenderova[104], J.W. Harris[144], A. Harton[11], H. Hassan[78], D. Hatzifotiadou[10,53], P. Hauer[42], S. Hayashi[130], S.T. Heckel[69], E. Hellbär[69], H. Helstrup[36], A. Herghelegiu[47], E.G. Hernandez[44], G. Herrera Corral[9], F. Herrmann[142], K.F. Hetland[36], T.E. Hilden[43], H. Hillemanns[34], C. Hills[127], B. Hippolyte[134], B. Hohlweger[103], D. Horak[37], S. Hornung[104], R. Hosokawa[78,131], J. Hota[66], P. Hristov[34], C. Huang[61], C. Hughes[128], P. Huhn[69], T.J. Humanic[95],

H. Hushnud[107], N. Hussain[41], T. Hussain[17], D. Hutter[39], D.S. Hwang[19], J.P. Iddon[127], R. Ilkaev[106], M. Inaba[131], M. Ippolitov[87], M.S. Islam[107], M. Ivanov[104], V. Ivanov[96], V. Izucheev[90], B. Jacak[79], N. Jacazio[27], P.M. Jacobs[79], M.B. Jadhav[48], S. Jadlovska[115], J. Jadlovsky[115], S. Jaelani[63], C. Jahnke[116,120], M.J. Jakubowska[140], M.A. Janik[140], C. Jena[85], M. Jercic[97], O. Jevons[108], R.T. Jimenez Bustamante[104], M. Jin[125], P.G. Jones[108], A. Jusko[108], P. Kalinak[65], A. Kalweit[34], J.H. Kang[145], V. Kaplin[91], S. Kar[6], A. Karasu Uysal[77], O. Karavichev[62], T. Karavicheva[62], P. Karczmarczyk[34], E. Karpechev[62], U. Kebschull[74], R. Keidel[46], D.L.D. Keijdener[63], M. Keil[34], B. Ketzer[42], Z. Khabanova[89], A.M. Khan[6], S. Khan[17], S.A. Khan[139], A. Khanzadeev[96], Y. Kharlov[90], A. Khatun[17], A. Khuntia[49], M.M. Kielbowicz[117], B. Kileng[36], B. Kim[131], D. Kim[145], D.J. Kim[126], E.J. Kim[13], H. Kim[145], J.S. Kim[40], J. Kim[102], J. Kim[13], M. Kim[60,102], S. Kim[19], T. Kim[145], T. Kim[145], K. Kindra[98], S. Kirsch[39], I. Kisel[39], S. Kiselev[64], A. Kisiel[140], J.L. Klay[5], C. Klein[69], J. Klein[58], C. Klein-Bösing[142], S. Klewin[102], A. Kluge[34], M.L. Knichel[34], A.G. Knospe[125], C. Kobdaj[114], M. Kofarago[143], M.K. Köhler[102], T. Kollegger[104], N. Kondratyeva[91], E. Kondratyuk[90], A. Konevskikh[62], P.J. Konopka[34], M. Konyushikhin[141], L. Koska[115], O. Kovalenko[84], V. Kovalenko[111], M. Kowalski[117], I. Králik[65], A. Kravčáková[38], L. Kreis[104], M. Krivda[65,108], F. Krizek[93], M. Krüger[69], E. Kryshen[96], M. Krzewicki[39], A.M. Kubera[95], V. Kučera[60,93], C. Kuhn[134], P.G. Kuijer[89], J. Kumar[48], L. Kumar[98], S. Kumar[48], S. Kundu[85], P. Kurashvili[84], A. Kurepin[62], A.B. Kurepin[62], S. Kushpil[93], J. Kvapil[108], M.J. Kweon[60], Y. Kwon[145], S.L. La Pointe[39], P. La Rocca[28], Y.S. Lai[79], I. Lakomov[34], R. Langoy[123], K. Lapidus[144], A. Lardeux[21], P. Larionov[51], E. Laudi[34], R. Lavicka[37], R. Lea[25], L. Leardini[102], S. Lee[145], F. Lehas[89], S. Lehner[112], J. Lehrbach[39], R.C. Lemmon[92], I. León Monzón[119], P. Lévai[143], X. Li[12], X.L. Li[6], J. Lien[123], R. Lietava[108], B. Lim[18], S. Lindal[21], V. Lindenstruth[39], S.W. Lindsay[127], C. Lippmann[104], M.A. Lisa[95], V. Litichevskyi[43], A. Liu[79], H.M. Ljunggren[80], W.J. Llope[141], D.F. Lodato[63], V. Loginov[91], C. Loizides[79,94], P. Loncar[35], X. Lopez[132], E. López Torres[8], P. Luettig[69], J.R. Luhder[142], M. Lunardon[29], G. Luparello[59], M. Lupi[34], A. Maevskaya[62], M. Mager[34], S.M. Mahmood[21], A. Maire[134], R.D. Majka[144], M. Malaev[96], Q.W. Malik[21], L. Malinina[III,75], D. Mal'Kevich[64], P. Malzacher[104], A. Mamonov[106], V. Manko[87], F. Manso[132], V. Manzari[52], Y. Mao[6], M. Marchisone[129,133], J. Mareš[67], G.V. Margagliotti[25], A. Margotti[53], J. Margutti[63], A. Marín[104], C. Markert[118], M. Marquard[69], N.A. Martin[102,104], P. Martinengo[34], J.L. Martinez[125], M.I. Martínez[44], G. Martínez García[113], M. Martinez Pedreira[34], S. Masciocchi[104], M. Masera[26], A. Masoni[54], L. Massacrier[61], E. Masson[113], A. Mastroserio[52,136], A.M. Mathis[103,116], P.F.T. Matuoka[120], A. Matyja[117,128], C. Mayer[117], M. Mazzilli[33], M.A. Mazzoni[57], F. Meddi[23], Y. Melikyan[91], A. Menchaca-Rocha[72], E. Meninno[30], M. Meres[14], S. Mhlanga[124], Y. Miake[131], L. Micheletti[26], M.M. Mieskolainen[43], D.L. Mihaylov[103], K. Mikhaylov[64,75], A. Mischke[63], A.N. Mishra[70], D. Miśkowiec[104], J. Mitra[139], C.M. Mitu[68], N. Mohammadi[34], A.P. Mohanty[63], B. Mohanty[85], M. Mohisin Khan[IV,17], D.A. Moreira De Godoy[142], L.A.P. Moreno[44], S. Moretto[29], A. Morreale[113], A. Morsch[34], T. Mrnjavac[34], V. Muccifora[51], E. Mudnic[35], D. Mühlheim[142], S. Muhuri[139], M. Mukherjee[3], J.D. Mulligan[144], M.G. Munhoz[120], K. Münning[42], R.H. Munzer[69], H. Murakami[130], S. Murray[73], L. Musa[34], J. Musinsky[65], C.J. Myers[125], J.W. Myrcha[140], B. Naik[48], R. Nair[84], B.K. Nandi[48], R. Nania[10,53], E. Nappi[52], A. Narayan[48], M.U. Naru[15], A.F. Nassirpour[80], H. Natal da Luz[120], C. Nattrass[128], S.R. Navarro[44], K. Nayak[85], R. Nayak[48], T.K. Nayak[139], S. Nazarenko[106], R.A. Negrao De Oliveira[34,69], L. Nellen[70], S.V. Nesbo[36], G. Neskovic[39], F. Ng[125], M. Nicassio[104], J. Niedziela[34,140], B.S. Nielsen[88], S. Nikolaev[87], S. Nikulin[87], V. Nikulin[96], F. Noferini[10,53], P. Nomokonov[75], G. Nooren[63], J.C.C. Noris[44], J. Norman[78], A. Nyanin[87], J. Nystrand[22], M. Ogino[81], H. Oh[145], A. Ohlson[102], J. Oleniacz[140], A.C. Oliveira Da Silva[120], M.H. Oliver[144], J. Onderwaater[104], C. Oppedisano[58], R. Orava[43], M. Oravec[115], A. Ortiz Velasquez[70], A. Oskarsson[80], J. Otwinowski[117], K. Oyama[81], Y. Pachmayer[102], V. Pacik[88], D. Pagano[138], G. Paić[70], P. Palni[6], J. Pan[141], A.K. Pandey[48], S. Panebianco[135], V. Papikyan[1], P. Pareek[49], J. Park[60], J.E. Parkkila[126], S. Parmar[98], A. Passfeld[142], S.P. Pathak[125], R.N. Patra[139], B. Paul[58], H. Pei[6], T. Peitzmann[63], X. Peng[6], L.G. Pereira[71], H. Pereira Da Costa[135], D. Peresunko[87], E. Perez Lezama[69], V. Peskov[69], Y. Pestov[4], V. Petráček[37], M. Petrovici[47], C. Petta[28], R.P. Pezzi[71], S. Piano[59], M. Pikna[14], P. Pillot[113], L.O.D.L. Pimentel[88], O. Pinazza[34,53], L. Pinsky[125], S. Pisano[51], D.B. Piyarathna[125], M. Płoskoń[79], M. Planinic[97], F. Pliquett[69], J. Pluta[140], S. Pochybova[143], P.L.M. Podesta-Lerma[119], M.G. Poghosyan[94], B. Polichtchouk[90], N. Poljak[97], W. Poonsawat[114], A. Pop[47], H. Poppenborg[142], S. Porteboeuf-Houssais[132], V. Pozdniakov[75], S.K. Prasad[3], R. Preghenella[53], F. Prino[58], C.A. Pruneau[141], I. Pshenichnov[62], M. Puccio[26], V. Punin[106], K. Puranapanda[139], J. Putschke[141], S. Raha[3], S. Rajput[99], J. Rak[126], A. Rakotozafindrabe[135], L. Ramello[32], F. Rami[134], R. Raniwala[100], S. Raniwala[100], S.S. Räsänen[43], B.T. Rascanu[69], R. Rath[49], V. Ratza[42], I. Ravasenga[31], K.F. Read[94,128], K. Redlich[V,84], A. Rehman[22], P. Reichelt[69], F. Reidt[34], X. Ren[6], R. Renfordt[69], A. Reshetin[62], J.-P. Revol[10], K. Reygers[102], V. Riabov[96], T. Richert[63,80,88], M. Richter[21], P. Riedler[34], W. Riegler[34], F. Riggi[28], C. Ristea[68], S.P. Rode[49], M. Rodríguez Cahuantzi[44], K. Røed[21], R. Rogalev[90], E. Rogochaya[75], D. Rohr[34], D. Röhrich[22], P.S. Rokita[140], F. Ronchetti[51], E.D. Rosas[70], K. Roslon[140], P. Rosnet[132], A. Rossi[29,56],

A. Rotondi[137], F. Roukoutakis[83], C. Roy[134], P. Roy[107], O.V. Rueda[70], R. Rui[25], B. Rumyantsev[75], A. Rustamov[86], E. Ryabinkin[87], Y. Ryabov[96], A. Rybicki[117], S. Saarinen[43], S. Sadhu[139], S. Sadovsky[90], K. Šafařík[34], S.K. Saha[139], B. Sahoo[48], P. Sahoo[49], R. Sahoo[49], S. Sahoo[66], P.K. Sahu[66], J. Saini[139], S. Sakai[131], M.A. Saleh[141], S. Sambyal[99], V. Samsonov[91,96], A. Sandoval[72], A. Sarkar[73], D. Sarkar[139], N. Sarkar[139], P. Sarma[41], M.H.P. Sas[63], E. Scapparone[53], F. Scarlassara[29], B. Schaefer[94], H.S. Scheid[69], C. Schiaua[47], R. Schicker[102], C. Schmidt[104], H.R. Schmidt[101], M.O. Schmidt[102], M. Schmidt[101], N.V. Schmidt[69,94], J. Schukraft[34], Y. Schutz[34,134], K. Schwarz[104], K. Schweda[104], G. Scioli[27], E. Scomparin[58], M. Šefčík[38], J.E. Seger[16], Y. Sekiguchi[130], D. Sekihata[45], I. Selyuzhenkov[91,104], S. Senyukov[134], E. Serradilla[72], P. Sett[48], A. Sevcenco[68], A. Shabanov[62], A. Shabetai[113], R. Shahoyan[34], W. Shaikh[107], A. Shangaraev[90], A. Sharma[98], A. Sharma[99], M. Sharma[99], N. Sharma[98], A.I. Sheikh[139], K. Shigaki[45], M. Shimomura[82], S. Shirinkin[64], Q. Shou[6,110], Y. Sibiriak[87], S. Siddhanta[54], K.M. Sielewicz[34], T. Siemiarczuk[84], D. Silvermyr[80], G. Simatovic[89], G. Simonetti[34,103], R. Singaraju[139], R. Singh[85], R. Singh[99], V. Singhal[139], T. Sinha[107], B. Sitar[14], M. Sitta[32], T.B. Skaali[21], M. Slupecki[126], N. Smirnov[144], R.J.M. Snellings[63], T.W. Snellman[126], J. Sochan[115], C. Soncco[109], J. Song[18,60], A. Songmoolnak[114], F. Soramel[29], S. Sorensen[128], F. Sozzi[104], I. Sputowska[117], J. Stachel[102], I. Stan[68], P. Stankus[94], E. Stenlund[80], D. Stocco[113], M.M. Storetvedt[36], P. Strmen[14], A.A.P. Suaide[120], T. Sugitate[45], C. Suire[61], M. Suleymanov[15], M. Suljic[34], R. Sultanov[64], M. Šumbera[93], S. Sumowidagdo[50], K. Suzuki[112], S. Swain[66], A. Szabo[14], I. Szarka[14], U. Tabassam[15], J. Takahashi[121], G.J. Tambave[22], N. Tanaka[131], M. Tarhini[113], M.G. Tarzila[47], A. Tauro[34], G. Tejeda Muñoz[44], A. Telesca[34], C. Terrevoli[29], B. Teyssier[133], D. Thakur[49], S. Thakur[139], D. Thomas[118], F. Thoresen[88], R. Tieulent[133], A. Tikhonov[62], A.R. Timmins[125], A. Toia[69], N. Topilskaya[62], M. Toppi[51], S.R. Torres[119], S. Tripathy[49], S. Trogolo[26], G. Trombetta[33], L. Tropp[38], V. Trubnikov[2], W.H. Trzaska[126], T.P. Trzcinski[140], B.A. Trzeciak[63], T. Tsuji[130], A. Tumkin[106], R. Turrisi[56], T.S. Tveter[21], K. Ullaland[22], E.N. Umaka[125], A. Uras[133], G.L. Usai[24], A. Utrobicic[97], M. Vala[115], L. Valencia Palomo[44], N. Valle[137], N. van der Kolk[63], L.V.R. van Doremalen[63], J.W. Van Hoorne[34], M. van Leeuwen[63], P. Vande Vyvre[34], D. Varga[143], A. Vargas[44], M. Vargyas[126], R. Varma[48], M. Vasileiou[83], A. Vasiliev[87], O. Vázquez Doce[103,116], V. Vechernin[111], A.M. Veen[63], E. Vercellin[26], S. Vergara Limón[44], L. Vermunt[63], R. Vernet[7], R. Vértesi[143], L. Vickovic[35], J. Viinikainen[126], Z. Vilakazi[129], O. Villalobos Baillie[108], A. Villatoro Tello[44], A. Vinogradov[87], T. Virgili[30], V. Vislavicius[80,88], A. Vodopyanov[75], M.A. Völkl[101], K. Voloshin[64], S.A. Voloshin[141], G. Volpe[33], B. von Haller[34], I. Vorobyev[103,116], D. Voscek[115], D. Vranic[34,104], J. Vrláková[38], B. Wagner[22], M. Wang[6], Y. Watanabe[131], M. Weber[112], S.G. Weber[104], A. Wegrzynek[34], D.F. Weiser[102], S.C. Wenzel[34], J.P. Wessels[142], U. Westerhoff[142], A.M. Whitehead[124], J. Wiechula[69], J. Wikne[21], G. Wilk[84], J. Wilkinson[53], G.A. Willems[34,142], M.C.S. Williams[53], E. Willsher[108], B. Windelband[102], W.E. Witt[128], R. Xu[6], S. Yalcin[77], K. Yamakawa[45], S. Yano[45,135], Z. Yin[6], H. Yokoyama[78,131], I.-K. Yoo[18], J.H. Yoon[60], S. Yuan[22], V. Yurchenko[2], V. Zaccolo[58], A. Zaman[15], C. Zampolli[34], H.J.C. Zanoli[120], N. Zardoshti[108], A. Zarochentsev[111], P. Závada[67], N. Zaviyalov[106], H. Zbroszczyk[140], M. Zhalov[96], X. Zhang[6], Y. Zhang[6], Z. Zhang[6,132], C. Zhao[21], V. Zherebchevskii[111], N. Zhigareva[64], D. Zhou[6], Y. Zhou[88], Z. Zhou[22], H. Zhu[6], J. Zhu[6], Y. Zhu[6], A. Zichichi[10,27], M.B. Zimmermann[34], G. Zinovjev[2], J. Zmeskal[112]

Affiliation Notes

[I] Deceased
[II] Also at: Dipartimento DET del Politecnico di Torino, Turin, Italy
[III] Also at: M.V. Lomonosov Moscow State University, D.V. Skobeltsyn Institute of Nuclear, Physics, Moscow, Russia
[IV] Also at: Department of Applied Physics, Aligarh Muslim University, Aligarh, India
[V] Also at: Institute of Theoretical Physics, University of Wroclaw, Poland

Collaboration Institutes

[1] A.I. Alikhanyan National Science Laboratory (Yerevan Physics Institute) Foundation, Yerevan, Armenia
[2] Bogolyubov Institute for Theoretical Physics, National Academy of Sciences of Ukraine, Kiev, Ukraine
[3] Bose Institute, Department of Physics and Centre for Astroparticle Physics and Space Science (CAPSS), Kolkata, India
[4] Budker Institute for Nuclear Physics, Novosibirsk, Russia

[5] California Polytechnic State University, San Luis Obispo, California, United States
[6] Central China Normal University, Wuhan, China
[7] Centre de Calcul de l'IN2P3, Villeurbanne, Lyon, France
[8] Centro de Aplicaciones Tecnológicas y Desarrollo Nuclear (CEADEN), Havana, Cuba
[9] Centro de Investigación y de Estudios Avanzados (CINVESTAV), Mexico City and Mérida, Mexico
[10] Centro Fermi - Museo Storico della Fisica e Centro Studi e Ricerche "Enrico Fermi', Rome, Italy
[11] Chicago State University, Chicago, Illinois, United States
[12] China Institute of Atomic Energy, Beijing, China
[13] Chonbuk National University, Jeonju, Republic of Korea
[14] Comenius University Bratislava, Faculty of Mathematics, Physics and Informatics, Bratislava, Slovakia
[15] COMSATS Institute of Information Technology (CIIT), Islamabad, Pakistan
[16] Creighton University, Omaha, Nebraska, United States
[17] Department of Physics, Aligarh Muslim University, Aligarh, India
[18] Department of Physics, Pusan National University, Pusan, Republic of Korea
[19] Department of Physics, Sejong University, Seoul, Republic of Korea
[20] Department of Physics, University of California, Berkeley, California, United States
[21] Department of Physics, University of Oslo, Oslo, Norway
[22] Department of Physics and Technology, University of Bergen, Bergen, Norway
[23] Dipartimento di Fisica dell'Università 'La Sapienza' and Sezione INFN, Rome, Italy
[24] Dipartimento di Fisica dell'Università and Sezione INFN, Cagliari, Italy
[25] Dipartimento di Fisica dell'Università and Sezione INFN, Trieste, Italy
[26] Dipartimento di Fisica dell'Università and Sezione INFN, Turin, Italy
[27] Dipartimento di Fisica e Astronomia dell'Università and Sezione INFN, Bologna, Italy
[28] Dipartimento di Fisica e Astronomia dell'Università and Sezione INFN, Catania, Italy
[29] Dipartimento di Fisica e Astronomia dell'Università and Sezione INFN, Padova, Italy
[30] Dipartimento di Fisica 'E.R. Caianiello' dell'Università and Gruppo Collegato INFN, Salerno, Italy
[31] Dipartimento DISAT del Politecnico and Sezione INFN, Turin, Italy
[32] Dipartimento di Scienze e Innovazione Tecnologica dell'Università del Piemonte Orientale and INFN Sezione di Torino, Alessandria, Italy
[33] Dipartimento Interateneo di Fisica 'M. Merlin' and Sezione INFN, Bari, Italy
[34] European Organization for Nuclear Research (CERN), Geneva, Switzerland
[35] Faculty of Electrical Engineering, Mechanical Engineering and Naval Architecture, University of Split, Split, Croatia
[36] Faculty of Engineering and Science, Western Norway University of Applied Sciences, Bergen, Norway
[37] Faculty of Nuclear Sciences and Physical Engineering, Czech Technical University in Prague, Prague, Czech Republic
[38] Faculty of Science, P.J. Šafárik University, Košice, Slovakia
[39] Frankfurt Institute for Advanced Studies, Johann Wolfgang Goethe-Universität Frankfurt, Frankfurt, Germany
[40] Gangneung-Wonju National University, Gangneung, Republic of Korea
[41] Gauhati University, Department of Physics, Guwahati, India
[42] Helmholtz-Institut für Strahlen- und Kernphysik, Rheinische Friedrich-Wilhelms-Universität Bonn, Bonn, Germany
[43] Helsinki Institute of Physics (HIP), Helsinki, Finland
[44] High Energy Physics Group, Universidad Autónoma de Puebla, Puebla, Mexico
[45] Hiroshima University, Hiroshima, Japan
[46] Hochschule Worms, Zentrum für Technologietransfer und Telekommunikation (ZTT), Worms, Germany
[47] Horia Hulubei National Institute of Physics and Nuclear Engineering, Bucharest, Romania
[48] Indian Institute of Technology Bombay (IIT), Mumbai, India
[49] Indian Institute of Technology Indore, Indore, India
[50] Indonesian Institute of Sciences, Jakarta, Indonesia
[51] INFN, Laboratori Nazionali di Frascati, Frascati, Italy
[52] INFN, Sezione di Bari, Bari, Italy
[53] INFN, Sezione di Bologna, Bologna, Italy
[54] INFN, Sezione di Cagliari, Cagliari, Italy
[55] INFN, Sezione di Catania, Catania, Italy
[56] INFN, Sezione di Padova, Padova, Italy

[57] INFN, Sezione di Roma, Rome, Italy
[58] INFN, Sezione di Torino, Turin, Italy
[59] INFN, Sezione di Trieste, Trieste, Italy
[60] Inha University, Incheon, Republic of Korea
[61] Institut de Physique Nucléaire d'Orsay (IPNO), Institut National de Physique Nucléaire et de Physique des Particules (IN2P3/CNRS), Université de Paris-Sud, Université Paris-Saclay, Orsay, France
[62] Institute for Nuclear Research, Academy of Sciences, Moscow, Russia
[63] Institute for Subatomic Physics, Utrecht University/Nikhef, Utrecht, Netherlands
[64] Institute for Theoretical and Experimental Physics, Moscow, Russia
[65] Institute of Experimental Physics, Slovak Academy of Sciences, Košice, Slovakia
[66] Institute of Physics, Homi Bhabha National Institute, Bhubaneswar, India
[67] Institute of Physics of the Czech Academy of Sciences, Prague, Czech Republic
[68] Institute of Space Science (ISS), Bucharest, Romania
[69] Institut für Kernphysik, Johann Wolfgang Goethe-Universität Frankfurt, Frankfurt, Germany
[70] Instituto de Ciencias Nucleares, Universidad Nacional Autónoma de México, Mexico City, Mexico
[71] Instituto de Física, Universidade Federal do Rio Grande do Sul (UFRGS), Porto Alegre, Brazil
[72] Instituto de Física, Universidad Nacional Autónoma de México, Mexico City, Mexico
[73] iThemba LABS, National Research Foundation, Somerset West, South Africa
[74] Johann-Wolfgang-Goethe Universität Frankfurt Institut für Informatik, Fachbereich Informatik und Mathematik, Frankfurt, Germany
[75] Joint Institute for Nuclear Research (JINR), Dubna, Russia
[76] Korea Institute of Science and Technology Information, Daejeon, Republic of Korea
[77] KTO Karatay University, Konya, Turkey
[78] Laboratoire de Physique Subatomique et de Cosmologie, Université Grenoble-Alpes, CNRS-IN2P3, Grenoble, France
[79] Lawrence Berkeley National Laboratory, Berkeley, California, United States
[80] Lund University Department of Physics, Division of Particle Physics, Lund, Sweden
[81] Nagasaki Institute of Applied Science, Nagasaki, Japan
[82] Nara Women's University (NWU), Nara, Japan
[83] National and Kapodistrian University of Athens, School of Science, Department of Physics , Athens, Greece
[84] National Centre for Nuclear Research, Warsaw, Poland
[85] National Institute of Science Education and Research, Homi Bhabha National Institute, Jatni, India
[86] National Nuclear Research Center, Baku, Azerbaijan
[87] National Research Centre Kurchatov Institute, Moscow, Russia
[88] Niels Bohr Institute, University of Copenhagen, Copenhagen, Denmark
[89] Nikhef, National institute for subatomic physics, Amsterdam, Netherlands
[90] NRC Kurchatov Institute IHEP, Protvino, Russia
[91] NRNU Moscow Engineering Physics Institute, Moscow, Russia
[92] Nuclear Physics Group, STFC Daresbury Laboratory, Daresbury, United Kingdom
[93] Nuclear Physics Institute of the Czech Academy of Sciences, Řež u Prahy, Czech Republic
[94] Oak Ridge National Laboratory, Oak Ridge, Tennessee, United States
[95] Ohio State University, Columbus, Ohio, United States
[96] Petersburg Nuclear Physics Institute, Gatchina, Russia
[97] Physics department, Faculty of science, University of Zagreb, Zagreb, Croatia
[98] Physics Department, Panjab University, Chandigarh, India
[99] Physics Department, University of Jammu, Jammu, India
[100] Physics Department, University of Rajasthan, Jaipur, India
[101] Physikalisches Institut, Eberhard-Karls-Universität Tübingen, Tübingen, Germany
[102] Physikalisches Institut, Ruprecht-Karls-Universität Heidelberg, Heidelberg, Germany
[103] Physik Department, Technische Universität München, Munich, Germany
[104] Research Division and ExtreMe Matter Institute EMMI, GSI Helmholtzzentrum für Schwerionenforschung GmbH, Darmstadt, Germany
[105] Rudjer Bošković Institute, Zagreb, Croatia
[106] Russian Federal Nuclear Center (VNIIEF), Sarov, Russia
[107] Saha Institute of Nuclear Physics, Homi Bhabha National Institute, Kolkata, India
[108] School of Physics and Astronomy, University of Birmingham, Birmingham, United Kingdom

[109] Sección Física, Departamento de Ciencias, Pontificia Universidad Católica del Perú, Lima, Peru
[110] Shanghai Institute of Applied Physics, Shanghai, China
[111] St. Petersburg State University, St. Petersburg, Russia
[112] Stefan Meyer Institut für Subatomare Physik (SMI), Vienna, Austria
[113] SUBATECH, IMT Atlantique, Université de Nantes, CNRS-IN2P3, Nantes, France
[114] Suranaree University of Technology, Nakhon Ratchasima, Thailand
[115] Technical University of Košice, Košice, Slovakia
[116] Technische Universität München, Excellence Cluster 'Universe', Munich, Germany
[117] The Henryk Niewodniczanski Institute of Nuclear Physics, Polish Academy of Sciences, Cracow, Poland
[118] The University of Texas at Austin, Austin, Texas, United States
[119] Universidad Autónoma de Sinaloa, Culiacán, Mexico
[120] Universidade de São Paulo (USP), São Paulo, Brazil
[121] Universidade Estadual de Campinas (UNICAMP), Campinas, Brazil
[122] Universidade Federal do ABC, Santo Andre, Brazil
[123] University College of Southeast Norway, Tonsberg, Norway
[124] University of Cape Town, Cape Town, South Africa
[125] University of Houston, Houston, Texas, United States
[126] University of Jyväskylä, Jyväskylä, Finland
[127] University of Liverpool, Liverpool, United Kingdom
[128] University of Tennessee, Knoxville, Tennessee, United States
[129] University of the Witwatersrand, Johannesburg, South Africa
[130] University of Tokyo, Tokyo, Japan
[131] University of Tsukuba, Tsukuba, Japan
[132] Université Clermont Auvergne, CNRS/IN2P3, LPC, Clermont-Ferrand, France
[133] Université de Lyon, Université Lyon 1, CNRS/IN2P3, IPN-Lyon, Villeurbanne, Lyon, France
[134] Université de Strasbourg, CNRS, IPHC UMR 7178, F-67000 Strasbourg, France, Strasbourg, France
[135] Université Paris-Saclay Centre dÉtudes de Saclay (CEA), IRFU, Department de Physique Nucléaire (DPhN), Saclay, France
[136] Università degli Studi di Foggia, Foggia, Italy
[137] Università degli Studi di Pavia and Sezione INFN, Pavia, Italy
[138] Università di Brescia and Sezione INFN, Brescia, Italy
[139] Variable Energy Cyclotron Centre, Homi Bhabha National Institute, Kolkata, India
[140] Warsaw University of Technology, Warsaw, Poland
[141] Wayne State University, Detroit, Michigan, United States
[142] Westfälische Wilhelms-Universität Münster, Institut für Kernphysik, Münster, Germany
[143] Wigner Research Centre for Physics, Hungarian Academy of Sciences, Budapest, Hungary
[144] Yale University, New Haven, Connecticut, United States
[145] Yonsei University, Seoul, Republic of Korea